A method for calculating the solar transmittance, absorptance and reflectance of a transparent insulation system

Wong, Ing Liang; Eames, Philip

Published in:
Solar Energy

DOI:
10.1016/j.solener.2014.09.028

Publication date:
2015

Document Version
Author accepted manuscript

A METHOD FOR CALCULATING THE SOLAR TRANSMITTANCE, ABSORPTANCE AND REFLECTANCE OF A TRANSPARENT INSULATION SYSTEM

Ing-Liang Wong[a1], Philip C Eames[b]

[a]School of Engineering and the Built Environment, Glasgow Caledonian University, 70 Cowcaddens Road, Glasgow, G4 0BA, UK (Email: IngLiang.Wong@gcu.ac.uk, xijiayu@hotmail.com; Tel: ++44(0)1413313864)

[b]CREST, Electronic and Electrical Engineering, Loughborough University, Leicester, LE11 3TU, UK (Email: P.C.Eames@lboro.ac.uk)

[1] Corresponding author

ABSTRACT

Transparent insulation materials (TIMs) can combine the advantages of opaque insulation with solar collection when applied to building facades. Mathematical models developed to calculate the optical performance of a transparent insulated (TI) system are presented. The TI-system modelled consisted of a 6mm outer glass pane, a 22mm wide polymethylmethacrylate (PMMA) capillary cell section and an 8mm inner glass pane. When solar beam radiation passed through the TI-system, the solar transmittance, absorptance and reflectance that occurred in the system were calculated. Optical interactions at each layer in the TI-system were numerically modelled for five incidence angles. A direct to diffuse transmittance was calculated for solar radiation passing through the PMMA capillary cells with an incidence angle, θ_i, in excess of 0°. The calculated transmittance for the PMMA capillary cells at 0° incidence angle was 0.8264 with overall solar transmittance of up to 0.66 calculated for the whole TI-system, a value which is consistent with that found in previous research. This paper presents a method for calculating the optical properties for multiple PMMA capillary cells, encapsulated between two glass panes for different solar incidence angles, with input of relevant data from other sources. This method can also be adapted for other types of glazing systems.

KEYWORDS

Solar transmittance; solar absorptance; solar reflectance; optical properties; transparent insulation materials; numerical modelling

1. INTRODUCTION

Prior to the term ‘transparent insulation’ being introduced, in 1929, Russian researchers introduced a honeycomb made of paper between the glass cover and absorber plate in a flat-plate solar collector, to investigate the possibility of using low-conducting and solar absorbing walls as a thermal insulation material (Veinburg, 1959). This was followed by the use of glass tubes in a solar collector perpendicular to the absorber, which were designed to work at high absorber temperatures (Francia, 1961). A theoretical study of honeycomb structures between absorber and outer glass cover of a flat-plate solar collector was performed to suppress convective heat transport (Hollands, 1965). Until 1969, plastic honeycombs with desired thermal characteristics and transparency were still not available for flat-plate solar collectors (Tabor, 1969). The earliest TIMs were used as absorbers or convection suppression devices (CSDs) in solar collectors and it was not until the 1980s, TIMs were used for building retrofits for energy conservation.

In the last 30 years, theoretical and experimental studies were performed to improve suppression of natural convection using large-celled and small-celled honeycomb structures. For examples, large-celled honeycomb structures made of highly transparent films, such as, fluorinated ethylene propylene (FEP), polypropylene, polycarbonate (PC) and fluorised films with U-values of approximately $2W/m^2K$ and working temperatures of between 60˚C and 100˚C were produced, commercialized, and used as CSDs for use in flat-plate collectors (Hollands et al., 1992; Platzer, 2001). Small-celled honeycomb structures made of glass or plastic, with square or circular cells, and improved optical and thermal properties (U-values of less than $1W/m^2K$), are easier to produce compared to large-celled honeycomb structures. The Fraunhofer

Institute for Solar Energy System (FISES) had pioneered this area of research using different materials to suppress heat transfer by convection and radiation (Platzer, 2001). The small-celled honeycomb structures produced commercially are made of polymethylmethacrylate (PMMA), PC, acrylic translucent foam, and aerogels. Their optical and thermal performance are both influenced by the uniformity and quality of the cells produced. The development of these small-celled honeycomb structures for application to building façades, mostly in cold climatic regions to reduce building heating and lighting loads (Wong et al., 2007), enables the heat loss through building envelopes to be reduced, while keep the thickness of the building facades to a minimum. TIMs can be applied to building facades as TI-wall (wall) and TI-glazing (window) systems. A TI-glazing system is formed when a layer of TIM is encapsulated between two glass panels; whilst, a TI-wall system requires a massive wall to be in place behind a TI-glazing to provide thermal mass/ storage. When used to replace standard opaque insulation materials, TI-systems not only perform similar functions to opaque insulation, such as, reduce heat losses and make indoor temperatures easier to control, the systems also allow solar transmittance of more than 50%.

Thermal and optical properties of TIMs made of different materials with different geometrical layouts have been determined theoretically, using mathematical models (Hollands, 1965; Hollands et al., 1978; Symons, 1982; Platzer, 1987; 1992a; 1992b; 1992c; Platzer and Kuehn, 1996; Arulanantham and Kaushika, 1994; Kaushika and Sumathy, 2003). The earliest theoretical model was developed to calculate angular dependent transmittance, $\tau(\theta)$, for a square honeycomb cell structure for various incidence angles, θ, taking into consideration cell thickness, depth and width (Hollands, 1965). Symons (1982) and Platzer (1987; 1992a; 1992b) developed a more precise model derived from the summation of all individual rays transmitted or reflected at the cell walls to calculate $\tau(\theta)$, taking into consideration the average number of cell wall interactions for the incoming light beam, n, azimuth angle, ϕ, reflectance, ρ, and absorptance, α, at the cell wall. An approximate model was developed to determine parameters required to fit $\tau(\theta)$ for ten different types of honeycombs and capillaries, taking into consideration surface imperfections and bulk effects of the cells. The model was based on an idealisation and does not consider real factors in the measured data, which are deviations from the idealised model (Platzer, 1992b). The values of $\tau(\theta)$ calculated using different analytical models agreed well for most TIMs for smaller incidence angles (Wong et al., 2007), albeit only for a limited number of TIM samples (Platzer, 1992a; 1992b).

Previous research has dealt with the calculation of optical properties for TIMs used in solar collectors. The development of TI-systems for building façade application, however, requires studies on whole systems, which include optical properties through glass layers. Despite Platzer and Kuehn (1996) calculating the optical properties of the combination of TIM and glass panes, there are gaps in knowledge about the energy performance of TI- systems due to lack of research analyzing the whole TI system, comprised of the TI material and enclosing glass panes. Building on the existing knowledge, we present numerical modelling studies to examine the optical properties of a TI-system, which includes PMMA capillary cells, encapsulated between two glass panes. This research provides a method for calculating the optical properties of a complete TI-system at any given incidence angle, with input of relevant data from other sources.

2. MODELLING OF A TI-SYSTEM

2.1. Description of the modelled TI-system

A 280mm high x 190mm wide, encapsulated KAPILUX Capillary System, which consists of a 6mm thick outer glass pane, a 22mm thick KAPIPANE slab and an 8mm thick inner glass pane, shown in Figure 1, was considered. The system, which was developed by OKALUX GmbH, consists of PMMA capillaries of approximately 2.5mm diameter, encapsulated between two panes of clear flat float glass, with properties shown in Table 1. Mathematical models were developed to calculate the optical properties of the TI-system when solar beam radiation was incident on the exterior glass surface at five angles of incidence, θ_i (0˚, 40˚, 55˚, 70˚ and 80˚). The values of optical properties calculated for the five angles reported in this paper provide sufficient information to interpolate values for other engles with reasonable accuracy. The overall solar transmittance for the TI-system and solar absorptivity at the glass panes and within the TIM slab were calculated and used in an energy simulation package, Environmental Systems Performance-research (ESP-r) for evaluating TIM system performance (Wong, 2007).

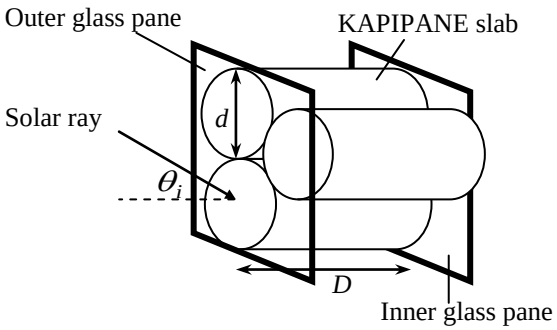

Figure 1 Illustration of the encapsulated TI-system

Parameters	Air space	Outer glass pane	Inner glass pane
Thickness, L (m)	-	0.006	0.008
Extinction coefficient, K (m^{-1})	-	4	4
Refractive indices, $\dot{n}$	1.000	1.526	1.526

Table 1 Properties of the glass pane covers used in the TI-system

2.2. Solar transmission through the outer glass pane

Figure 2 shows the incoming solar radiation passing through the outer glass pane of the system. The angles of incidence, θ_i and refraction, θ_r, at the outer glass pane were defined as θ_1 and θ_3, as well as θ_2 and θ_4. The intensity of direct solar radiation incident on the outer glass pane is equal to 1, ρ_{ou} is reflected, α_{ou} is absorbed, and the fraction of 1-ρ_{ou}-α_{ou} is transmitted through the glass pane, which is assumed to be τ_{ou}. Table 2 shows the calculated θ_i and θ_r, using $\frac{\dot{n}_{air}}{\dot{n}_{\text{glass}}} = \frac{\sin\theta_r}{\sin\theta_i}$ as expressed in Snell's Law.

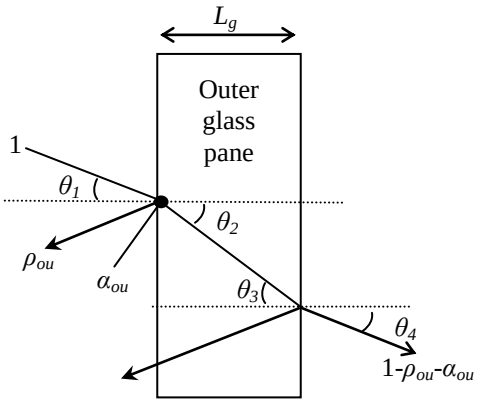

Figure 2 Light transmission, absorption and reflection at the outer glass pane

θ_1 (°)	θ_2 (°)	θ_3 (°)	θ_4 (°)
0	0	0	0
40	24.91	24.91	40
55	32.47	32.47	55
70	38.01	38.01	70
80	40.19	40.19	80

Table 2 Angles of incidence and refraction of the outer glass cover

The unpolarised solar radiation can be divided into perpendicular and parallel components, $r_\perp$ and r_{II} (Duffie and Beckman, 1991), which can be determined by Eqs. (1) and (2).

$$r_\perp = \frac{\sin^2(\theta_r - \theta_i)}{\sin^2(\theta_r + \theta_i)} \tag{1}$$

$$r_{II} = \frac{\tan^2(\theta_r - \theta_i)}{\tan^2(\theta_r + \theta_i)} \tag{2}$$

The reflectance of the unpolarised radiation can be calculated as the average of $r_\perp$ and r_{II} and determined by

$$\rho = \frac{1}{2}(r_\perp + r_{II}) \tag{3}$$

For solar radiation at normal incidence, both θ_i and θ_r are zero and the reflectance was calculated using

$$\rho = \left(\frac{\dot{n}_{air} - \dot{n}_{glass}}{\dot{n}_{air} + \dot{n}_{glass}} \right)^2 \tag{4}$$

Using θ_i and θ_r calculated in Table 2, $r_\perp$, r_{II} and ρ were determined by Eqs. (1) to (3) and are shown in Table 3.

Angles of incidence, θ_1 (°)	$r_\perp$	r_{II}	ρ
0	-	-	0.0434
40	0.0827	0.0159	0.0493
55	0.1471	0.000336	0.0737
70	0.3104	0.0412	0.1758
80	0.5487	0.2351	0.3919

Table 3 Perpendicular ($r_\perp$) and parallel (r_{II}) components and reflectance (ρ) of unpolarised solar radiation at different angles of incidence (θ_1)

In the calculations of transmittance of unpolarised solar radiation through the outer glass cover, both reflection and absorption losses should be taken into consideration (Duffie and Beckman, 1991). The transmittance, which takes into consideration reflection loss ($\tau_{reflect}$), was determined by Eq. (5). For solar radiation at normal incidence, $\tau_{reflect}$ was determined by Eq. (6); while the transmittance, which takes into consideration absorption loss (τ_{absorp}), was determined by Eq. (7).

$$\tau_{reflect} = \frac{1}{2}\left(\frac{1-r_{II}}{1+r_{II}} + \frac{1-r_\perp}{1+r_\perp}\right) \tag{5}$$

$$\tau_{reflect} = \frac{1-\rho}{1+\rho} \tag{6}$$

$$\tau_{absorp} = \exp\left(-\frac{KL_g}{\cos\theta_r}\right) \tag{7}$$

The calculated transmittance (τ_{ou}), absorptance (α_{ou}) and reflectance (ρ_{ou}) of the outer glass pane were determined by Eqs. (8) to (10).

$$\tau_{ou} = \tau_{absorp}\tau_{reflect} \tag{8}$$

$$\alpha_{ou} = 1-\tau_{absorp} \tag{9}$$

$$\rho_{ou} = \tau_{absorp}-\tau_{ou} \tag{10}$$

2.3. Solar transmission from the outer glass pane to a single PMMA capillary cell

A typical optical behavior for a ray transmitted through the outer glass pane, τ_{ou}, was analysed when passing through a PMMA capillary cell with a hydraulic diameter, *d* and a cell wall thickness, *δ*. As shown in Figure 3, the angles of incidence and refraction at the cell wall were ϕ_i and ϕ_r, where, $\phi_i = \frac{\pi}{2} - \theta_1$ or 90° - θ_1. Figure 4 illustrates a solar ray

passing through a layer of capillary cell wall, with ϕ_i (ϕ_1 and ϕ_3) and ϕ_r (ϕ_2 and ϕ_4) at the cell wall. When τ_{ou} hits the wall of the first layer of the capillary cell, ρ_{cap} is reflected and α_{cap} is absorbed. The remaining τ_{cap} is transmitted through the cell wall to the adjacent capillary cell.

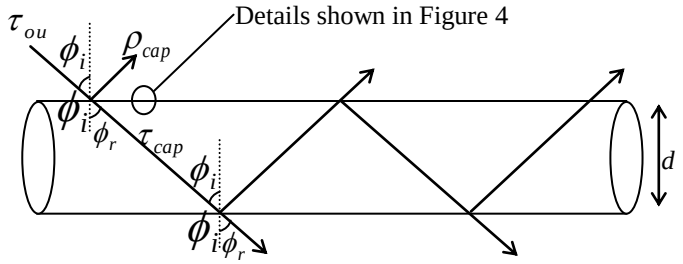

Figure 3 Multiple light reflection (ρ_{cap}) and transmission (τ_{cap}) through a PMMA capillary cell at angles of incidence (ϕ_i) and refraction (ϕ_r)

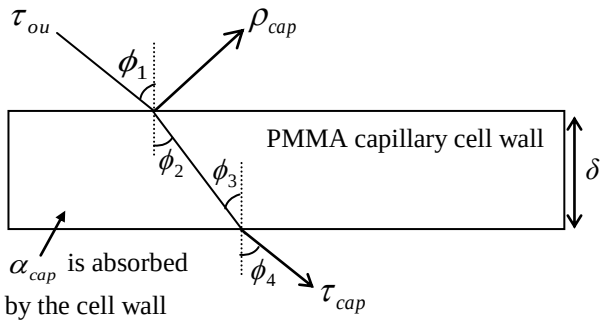

Figure 4 Solar transmittance (τ_{cap}), reflection (ρ_{cap}) and absorption (α_{cap}) through a PMMA capillary cell wall at incident (ϕ_1 and ϕ_3) and refraction (ϕ_2 and ϕ_4) angles

Table 4 shows the angles of incidence and refraction at PMMA cell, determined by Eq. (11). The extinction coefficient, *K*, of the PMMA capillary cell, was calculated using the equation developed by Platzer [11] to calculate inverse extinction coefficient, K^{-1} of the similar capillary cell. The fit coefficients, c_0 and c_1, refractive index, $\dot{n}_{cap}$, cell wall thickness (δ), density, diameter (*d*) and thickness (*D*) of the capillary cell are shown in Table 5.

$$\frac{\dot{n}_{air}}{\dot{n}_{\mathrm{cap}}} = \frac{\sin\phi_r}{\sin\phi_i} \tag{11}$$

Angles of incidence, θ_1 (°)	ϕ_1 (°)	ϕ_2 (°)	ϕ_3 (°)	ϕ_4 (°)
0	90	42.16	42.16	90
40	50	30.94	30.94	50
55	35	22.64	22.64	35
70	20	13.27	13.27	20
80	10	6.69	6.69	10

Table 4 Angles of reflection (ϕ_1 and ϕ_3) and refraction (ϕ_2 and ϕ_4) of PMMA capillary cell

Parameters	PMMA Cell	References
Wall thickness, δ (m)	0.000125	Wallner et al. (1999); OKALUX GmbH
Density (kg/m^3)	30	OKALUX GmbH
Cell diameter, d (m)	0.0025	OKALUX GmbH
Cell thickness, D (m)	0.022	OKALUX GmbH
Refractive index, $\dot{n}_{cap}$	1.49	Duffie and Beckman (1991)
Fit coefficient, c_0 (cm)	1.451 ± 0.046	Platzer (1992a)
Fit coefficient, c_1 (cm^{-1})	0.333 ± 0.037	Platzer (1992a)
Inverse extinction coefficient, K^{-1} (m)	0.0075	
Extinction coefficient, K (m^{-1})	133	

Table 5 Properties of the PMMA Capillary cell used in KAPILUX System

To calculate the reflectance (ρ_{cap}), absorptance (α_{cap}) and transmittance (τ_{cap}) of a PMMA capillary cell at an incidence angle of over 0°, the steps for calculating τ_{ou}, α_{ou} and ρ_{ou} of the outer glass cover using Eqs. (1) – (10) were repeated. The transmittance through the cell, which takes into consideration absorption loss, $\tau_{cap\ \ absorp}$, was determined by Eq. (12); while, ρ_{cap}, α_{cap} and τ_{cap} were determined by Eqs. (13) to (15).

$$\tau_{cap\ \ absorp} = \exp\left(-\frac{K\delta}{\cos\phi_r}\right) \tag{12}$$

$$\tau_{cap} = \tau_{cap\ \ absorp}\tau_{reflect} \tag{13}$$

$$\alpha_{cap} = 1 - \tau_{cap\ \ absorp} \tag{14}$$

$$\rho_{cap} = \tau_{cap\ \ absorp} - \tau_{cap} \tag{15}$$

The above steps, however, were inappropriate for calculating solar transmission for a value of θ_1 equals 0°. Hollands and co-researchers (Hollands et al., 1978) reported that, for θ_1 equals 0°, the value of ϕ_1 is 90° and a fraction of the solar radiation transmitted through the outer glass cover, τ_{ou}, will either enter the capillary cell or strike the top of the cell walls. A precise estimation of the transmission of light that hit the top of the cell walls, however, was not necessary (Hollands et al., 1978). Thus, it was assumed that, the radiation entering from the top of a cell wall is completely reflected internally at the cell wall due to a thin cell wall (δ = 0.125mm). Symons (1982) concluded that, at the incidence angle of 0°, the solar transmittance to beam radiation must be equal to or greater than the calculated ratio of void area to total area in the plane of capillary tube. Figure 5 shows the cross section of a capillary cell, indicating the wall thickness and diameter of the cell. The calculated the ratio of void area to the total area in the plane of a capillary cell was 0.8264, assuming the voids between adjacent tube walls are negligible. Thus, the transmittance through the capillary cell, τ_{cap}, at the θ_1 of 0° (i.e. the

light passing through the space between the cell walls) was 0.8264. Using Eqs. (13) to (15), τ_{cap}, α_{cap} and ρ_{cap} at the θ_1 other than 0° were calculated.

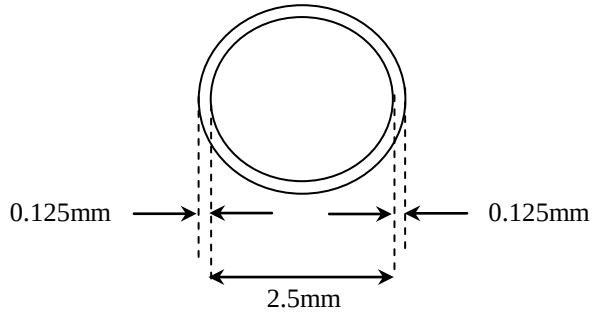

Figure 5 Cross section of a 2.5mm diameter KAPIPANE capillary cell with the cell wall of 0.125mm thick

2.4. Solar transmission through multiple PMMA capillary cells

The optical performance of multiple PMMA capillary cells was influenced by the geometrical layout of the material. Figure 6 shows the ray trace for a solar ray passing through different layers of cell walls. When a solar ray was transmitted through multiple PMMA capillary cells at an incidence angle of θ_i, a direct to diffuse transmittance was predicted. The solar ray was either reflected or transmitted towards the inner glass pane, resulting in scattering of the light over a large area. The solar radiation passing through the capillary cells intercepts with numerous cell walls. At each interception point, ρ_{cap} was reflected and α_{cap} was absorbed, whereas, the remaining τ_{cap} was transmitted to the adjacent cell. τ, α, and ρ were used in Figure 6 to represent τ_{ou}, α_{cap}, and ρ_{cap}. When a solar ray, τ, passes through a layer of capillary cell wall, at the first interception point, $\tau\alpha$ is absorbed, while $\tau\rho$ is reflected back to the cell wall. The solar radiation transmitted through the cell wall can be written as τ-$\tau\alpha$-$\tau\rho$ or $\tau(1\text{-}\alpha\text{-}\rho)$. Subsequently, the remaining solar beam radiation is incident at the 2nd, 3rd, 4th, until the nth cell walls, with components being absorbed and reflected at each intersection. The optical behaviour of the beam radiation for multiple interception points is shown in Figure 6.

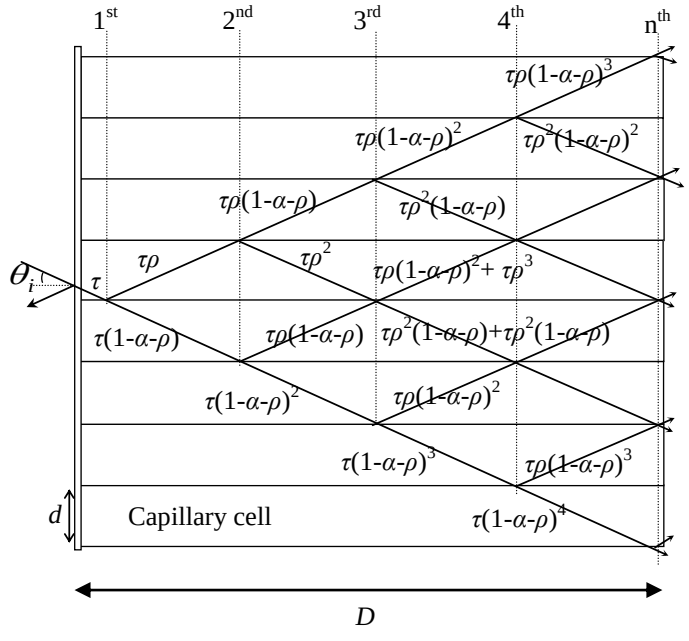

Figure 6 Multiple light reflection (ρ), absorption (α) and transmission (τ) of PMMA capillary cells

The average number of interception points, *n*, with the cell wall of the incoming solar beam, varies with θ_i and can be calculated using the equation $n = 2A\tan\theta_i$ (Symons, 1982), where, *A* is the aspect ratio of the capillary cell structure and can be defined as $\frac{D}{d}$; thus, *A* equal to 8.8 for the modelled system. At the 2nd interception point, the solar beam radiation intercepts with two cell walls, where, absorptance can be expressed as $\tau\rho\alpha + \tau\alpha(1-\alpha-\rho)$, reflectance can be expressed as $\tau\rho^2 + \tau\rho(1-\alpha-\rho)$, and transmittance can be expressed as $\tau(1-\alpha-\rho)^2 + \tau\rho(1-\alpha-\rho)$. The light transmittance at each interception point was calculated as the summation of all transmittance and reflectance at the interception point. Table 6 shows the summation of light transmittance and reflectance for the 1st, 2nd, 3rd, 4th and nth interception points for multiple PMMA capillary cells. The coefficients in front of the equations were derived from the summation of all transmittance and reflectance, which follows the rules of Pascal's Triangle, summarised in Table 7.

Interception points	1st	2nd	3rd	4th	…..	nth
Total transmittance and reflectance	$\tau\rho$	$\tau\rho^2$	$\tau\rho^3$	$\tau\rho^4$	…..	$\tau\rho^n$
	$\tau(1-\alpha-\rho)$	$\tau(1-\alpha-\rho)^2$	$\tau(1-\alpha-\rho)^3$	$\tau(1-\alpha-\rho)^4$		$\tau(1-\alpha-\rho)^n$
		$2\tau\rho(1-\alpha-\rho)$	$3\tau\rho(1-\alpha-\rho)^2$	$4\tau\rho(1-\alpha-\rho)^3$		$n\tau\rho(1-\alpha-\rho)^{n-1}$
			$3\tau\rho^2(1-\alpha-\rho)$	$6\tau\rho^2(1-\alpha-\rho)^2$		$Z_1\tau\rho^2(1-\alpha-\rho)^{n-2}$
				$4\tau\rho^3(1-\alpha-\rho)$		$Z_2\tau\rho^3(1-\alpha-\rho)^{n-3}$
						$Z_3\tau\rho^{n-1}(1-\alpha-\rho)^{n-x}$

Table 6 Total transmittance and reflectance at various interception points of PMMA capillary cells

2nd	3rd	4th	5th	6th	7th	8th	9th	10th	11th	12th	…..	nth
2	3	4	5	6	7	8	9	10	11	12	…..	*n*
	3	6	10	15	21	28	36	45	55	66	…..	Z_1
		4	10	20	35	56	84	120	165	220	…..	Z_2
			5	15	35	70	126	210	330	495	…..	Z_3
				6	21	56	126	252	462	792	…..	…..
					7	28	84	210	462	924	…..	Z_{ind}
						8	36	120	330	792	…..	…..
							9	45	165	495	…..	Z_3
								10	55	220	…..	Z_2
									11	66	…..	Z_1
										12	…..	*n*

Table 7 Summary of the coefficients in front of the equations derived for transmission and reflection that follow the rules of Pascal's Triangle

It was assumed that, at the nth interception point, the coefficient are Z_1, Z_2, Z_3, …. Z_{ind} ,which, Z_{ind} is coefficient at the nth point (indefinite). The light transmittance was calculated as the summation of all transmittance and reflectance, expressed by Eq. (16), where, *v* is an integer smaller than *n* and $n-v$ is greater than or equal to 1.

$$\tau\rho^{n} + \tau(1-\alpha-\rho)^{n} + n\tau\rho(1-\alpha-\rho)^{n-1} + Z_1\tau\rho^{2}(1-\alpha-\rho)^{n-2} + Z_2\tau\rho^{3}(1-\alpha-\rho)^{n-3} + Z_3\tau\rho^{4}(1-\alpha-\rho)^{n-4}$$
$$+ Z_4\tau\rho^{5}(1-\alpha-\rho)^{n-5} + \ldots\ldots + Z_{ind}\tau\rho^{n-1}(1-\alpha-\rho)^{n-v} \quad (16)$$

Table 8 shows the solar absorptance at various interception points, which can be divided into two components and represented by the presented series of equations. The first series of equations are $\tau\alpha + \tau\rho\alpha + \tau\rho^{2}\alpha + \tau\rho^{3}\alpha + \tau\rho^{4}\alpha + \tau\rho^{5}\alpha + \ldots\ldots\ldots + \tau\rho^{n-1}\alpha$ and the second series of equations are $\tau\alpha(1-\alpha-\rho) + \tau\alpha(1-\alpha-\rho)^{2} + \tau\alpha(1-\alpha-\rho)^{3} + \tau\alpha(1-\alpha-\rho)^{4} + \tau\alpha(1-\alpha-\rho)^{5} + \ldots\ldots\ldots + \tau\alpha(1-\alpha-\rho)^{n-1}$. The first to n[th] equations can be summed using equation $S_n = f\left(\frac{1-j^{n}}{1-j}\right)$, where, *f*, is represented by the first equation and *j* is the term given by dividing the second equation by the first equation.

Interception points	1st	2nd	3rd	4th	…..	nth
Total absorptance	$\tau\alpha$	$\tau\rho\alpha$	$\tau\rho^{2}\alpha$	$\tau\rho^{3}\alpha$	…..	$\tau\rho^{n-1}\alpha$
		$\tau\alpha(1-\alpha-\rho)$	$\tau\alpha(1-\alpha-\rho)^{2}$	$\tau\alpha(1-\alpha-\rho)^{3}$		$\tau\alpha(1-\alpha-\rho)^{n-1}$
			$2\tau\rho\alpha(1-\alpha-\rho)$	$3\tau\rho\alpha(1-\alpha-\rho)^{2}$		$Z_1\tau\rho\alpha(1-\alpha-\rho)^{n-2}$
				$3\tau\rho^{2}\alpha(1-\alpha-\rho)$		$Z_2\tau\rho^{2}\alpha(1-\alpha-\rho)^{n-3}$
						$Z_{ind}\tau\rho^{n-2}\alpha(1-\alpha-\rho)$

Table 8 Total solar absorptance at various interception points in PMMA capillary cells

The first series can be expressed by Eq. (17).

$$\tau\alpha\left[\frac{1-\rho^{n}}{1-\rho}\right] \quad (17)$$

The second series can be expressed by Eq. (18).

$$\tau\alpha(1-\alpha-\rho)\left[\frac{1-(1-\alpha-\rho)^{n-1}}{1-(1-\alpha-\rho)}\right] \quad (18)$$

The total absorptance at the capillary cells was calculated by summing up the absorptance at each interception point, which is given by Eq. (19), where, Z_1, Z_2, Z_3, ... Z_{ind} are coefficient that follows the rules of Pascal's Triangle (Table 7), at the n[th] interception point.

$$\tau\alpha\left[\frac{1-\rho^{n}}{1-\rho}\right] + \tau\alpha(1-\alpha-\rho)\left[\frac{1-(1-\alpha-\rho)^{n-1}}{1-(1-\alpha-\rho)}\right] + Z_1\tau\rho\alpha(1-\alpha-\rho)^{n-2} + Z_2\tau\rho^{2}\alpha(1-\alpha-\rho)^{n-3} +$$
$$Z_3\tau\rho^{3}\alpha(1-\alpha-\rho)^{n-4} + Z_4\tau\rho^{4}\alpha(1-\alpha-\rho)^{n-5} + \ldots\ldots\ldots + Z_{ind}\tau\rho^{n-2}\alpha(1-\alpha-\rho) \quad (19)$$

2.5. Solar transmission to the inner glass pane

The inner glass pane has the same physical properties as the outer glass pane, except that the thickness of the inner glass pane was 8mm. The calculations of the optical properties of the glass pane were repeated following the same procedure as for the outer glass pane.

3. RESULTS AND DISCUSSIONS

The solar transmittance, absorptance and reflectance when solar beam radiation passes through the outer glass pane, single and multiple capillary cells and the inner glass pane of a TI-system were calculated using Eqs. (8) to (10), (13) to (16), and (19). The calculated reflectance, absorptance and transmittance of the outer glass pane (ρ_{ou}, α_{ou} and τ_{ou}), a single PMMA capillary cell (ρ_{cap}, α_{cap} and τ_{cap}), multiple PMMA capillary cells and the inner glass pane (ρ_{in}, α_{in} and τ_{in}) at various values of θ_1, are shown in Table 9. The calculated transmittance and reflectance of the PMMA capillary cells at 0° was 0.8264, which agree well with the previous experimental results ranging from 0.8 to 0.96 for various types of PMMA capillary and honeycomb cells with various thicknesses (Platzer, 1992a; 1992b; 1992c). The summation of total light transmittance, reflectance and absorptance of PMMA capillary cells at any angle of incidence equals one, which indicates that the calculation procedure is self-consistent.

θ_1 (°)	n	Outer glass pane			A single PMMA capillary cell			Multiple PMMA capillary cells		Inner glass pane		
		τ_{ou}	α_{ou}	ρ_{ou}	τ_{cap}	α_{cap}	ρ_{cap}	Transmittance and reflectance	Total absorptance	τ_{in}	α_{in}	ρ_{in}
0	0	0.9022	0.0159	0.0819	0.8264	0.0222	0.1514	0.8264	0.1736	0.8879	0.0315	0.0806
40	15	0.8921	0.0175	0.0904	0.8812	0.0192	0.0996	0.7477	0.2523	0.8765	0.0347	0.0888
55	25	0.8550	0.0188	0.1262	0.9042	0.0179	0.0779	0.6366	0.3634	0.8390	0.0372	0.1238
70	48	0.7091	0.0201	0.2708	0.9096	0.0169	0.0735	0.4413	0.5587	0.6948	0.0398	0.2654
80	100	0.5086	0.0207	0.4707	0.9107	0.0166	0.0727	0.1875	0.8125	0.4981	0.0410	0.4609

Table 9 Solar transmittance, reflectance and absorptance of the outer glass pane, a single and multiple PMMA capillary cells and the inner glass pane at the five selected incidence angles (θ_1)

Using the individual transmittance calculated for the outer glass pane, PMMA capillary cells, and inner glass pane with the presented mathematical models, the direct to diffuse solar transmittance through the entire TI-system was calculated by evaluating and multiplying each individual transmittance to give a combined transmittance value. Table 10 shows the summary of the overall solar transmittance through the entire TI-system, with a transmittance of up to 66% achieved at the θ_1 of 0°.

θ_1 (°)	Transmittance & Reflectance			
	Outer glass, τ_{ou}	PMMA capillary slab	Inner glass, τ_{in}	Entire TI-system
0	0.9022	0.8264	0.8879	0.6620
40	0.8921	0.7477	0.8765	0.5846
55	0.8550	0.6366	0.8390	0.4567
70	0.7091	0.4413	0.6948	0.2174
80	0.5086	0.1875	0.4981	0.0475

Table 10 Solar transmittance through the entire TI-system at the five selected incidence angles (θ_1)

This research presents a novel numerical modelling technique for calculating the direct to diffuse, angular dependent transmittance, absorptance, and reflectance for different layers of a complicated TI-system, which consisted of a 6mm outer glass pane, a 22mm wide PMMA capillary slab and an 8mm inner glass pane. Compared to the models presented in the previous literature (Platzer, 1987; 1992a; 1992b; Buchberg et al., 1971), which were developed to calculate the optical properties for TIM layer only, the models presented in this research are more precise and capable of performing calculations of optical properties for different layers of the TI-system at any given angle of incidence. The results of this work are valuable for the determination of the energy performance of TI-systems, prior to application on to building facades. To examine the validity of the above calculations, the calculated results were compared with the results calculated using different models presented in the previous literature. Figure 7 shows the comparison of the values of direct-diffuse transmittance at different angles, $\tau(\theta)$, for different TIM layers calculated using numerical models presented in the previous literature (Platzer, 1987; 1992a; 1992b; Buchberg et al., 1971). The values of total transmittance and reflectance of the 22mm PMMA capillary slab determined by Eq. (16) (see Table 9) are also presented in the figure for comparison.

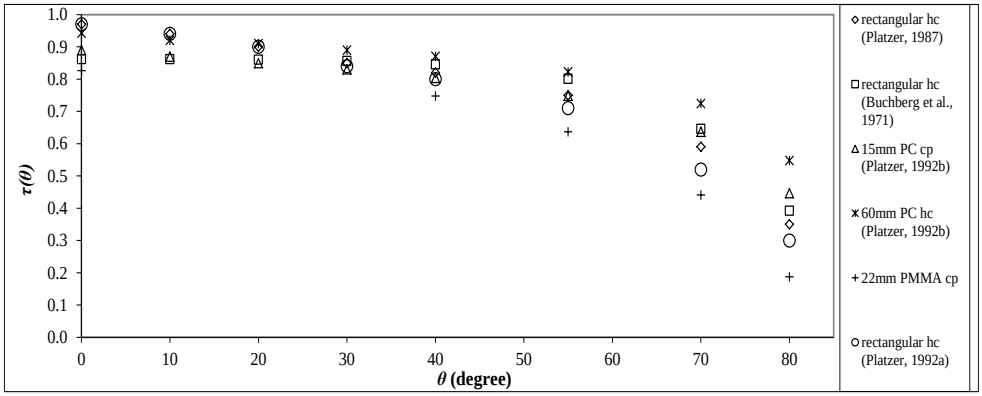

Figure 7 Comparison of direct-diffuse transmittance, $\tau(\theta)$ calculation with previous numerical models for rectangular honeycomb (hc), polycarbonate (PC) capillary (cp), PC honeycomb and PMMA capillary

The figure clearly illustrates that, the values of $\tau(\theta)$ calculated using different analytical models agreed well for smaller incidence angles. Despite theoretical calculations that indicate high $\tau(\theta)$ of more than 90% for most TIMs, when θ is 0˚, this value decreases dramatically after 70˚, which is in agreement with the previous experimental results (Wong et al., 2007), which showed $\tau(\theta)$ of more than 90% for θ in the range of 0 to 60˚. Transmittance differences among these calculations were found to be significant at higher angles of incidence. A limitation in this comparison is that, the previous models were not general, being developed for a number of TIM samples (Platzer, 1992a; 1992b), each with different structural arrangements, slab thicknesses, and physical properties.

4. CONCLUSIONS

This paper presents a novel method for calculating the optical properties for multiple PMMA capillary cells, encapsulated between two glass panes for different solar incidence angles. The direct to diffuse solar transmittance and absorptance at

each TI-system layer was calculated using the developed mathematical models with input of relevant data from other sources. Compared to the results obtained from the experimental work using similar types of capillary cells, the calculated values of transmittance, reflectance and obsorptance were consistent and in good agreement confirming the appropriateness and accuracy of the modelling approach developed. Thus, the developed calculation procedure was reasonably justified as the calculated solar transmittance was consistent with previous experimental results.

5. NOMENCLATURE

A	aspect ratio
c_0, c_1	fit coefficients for honeycomb structure (cm^{-1})
d	hydraulic diameter (mm)
D	thickness/ length of capillary cell (m)
f	first equation of series of equations
j	difference of second over the first equation
K	extinction coefficient (m^{-1})
n	number of cell walls that intersect with a light beam
$\dot{n}$	index of refraction
S_n	summation of 1st to nth equations
v	integer
$Z_{1,2,...ind}$	coefficient
ρ	solar reflectance (%)
τ	solar transmittance (%)
α	solar absorptance (%)
θ	solar incidence angle (˚)
ϕ	azimuth angle (˚)
δ	thickness of capillary cell wall (m)
L	thickness of glass pane (m)
r	unpolarised solar radiation
K^{-1}	inverse extinction coefficient (m)

Subscripts

i	incidence
ind	indefinite
r	refraction
ou	outer
absorp	absorptance
reflect	reflectance
cap	capillary cell
k	KAPIPANE

in	inner
g	glass
$\perp$	perpendicular
$\parallel$	parallel

6. REFERENCES

Arulanantham, M., Kaushika, N.D., 1994. Global radiation transmittance of transparent insulation materials. Solar Energy. 53(4), 323-328.

Buchberg, H., Lalude, O.A., Edwards, D.K., 1971. Performance characteristics of rectangular honeycomb solar–thermal converters. Solar Energy. 13, 193–221.

Duffie, J.A., Beckman, W.A., 1991. Solar Engineering of Thermal Processes, second ed. John Wiley and Sons, Inc, New York.

Francia, G., 1961. A new collector of solar radiant energy: theory and experimental verification. In: Proceedings of the United Nations Conference on New Sources of Energy, Rome, pp. 21-23.

Hollands, K.G.T., 1965. Honeycomb devices in flat plate solar collectors. Solar Energy. 9(3), 159-164.

Hollands, K.G.T., Iynkaran, K., Ford, C., Platzer, W.J., 1992. Manufacture, solar transmission and heat transfer characteristic of large-celled honeycomb transparent insulation. Solar Energy. 49(5), 381-386.

Hollands, K.G.T., Marshall, K.N., Wedel, R.K., 1978. An approximate equation for predicting the solar transmittance of transparent honeycombs. Solar Energy. 21, 231-236.

Kaushika, N.D., Sumathy, K.,2003. Solar transparent insulation materials: a review. Renewable and Sustainable Energy Reviews. 7(4), 317-351.

Platzer, W.J., 1987. Solar transmittance of transparent insulation materials. Solar Energy Materials. 16, 275-287.

Platzer, W.J., 1992a. Calculation Procedure for Collectors with a Honeycomb Cover of Rectangular Cross Section. Solar Energy. 48(6), 381-393.

Platzer, W.J., 1992b. Directional-hemispherical solar transmittance data for plastic type honeycomb structures. Solar Energy. 49(5), 359-369.

Platzer, W.J., 1992c. Total heat transport data for plastic honeycomb-type structures. Solar Energy. 49(5), 351-358.

Platzer, W.J., 2001. Transparent insulation materials and products: a review. Advances in Solar Energy. 14, 33-65.

Platzer, W.J., Kuehn, S., 1997. Calculation of heat transport and total solar energy transmittance from spectral optical data. In: Proceedings of the 8th International Meeting on Transparent Insulation Technology - TI8, Freiburg (editor: A. Goetzberger *et al*.), The Franklin Company Consultants Ltd., Birmingham.

Symons, J.G., 1982. The Solar Transmittance of Some Convection Suppression Devices for Solar Energy Applications: An Experimental Study. Journal of Solar Energy Engineering. 104, 251-256.

Tabor, H., 1969. Cellular insulation (honeycombs). Solar Energy. 12(4), 549-552.

Veinberg, V.B., 1959. Optics in equipment for the utilization of solar energy, State Publishing House of Defense Ministry, Moscow.

Wallner, G., Schobermayr, H., Lang, R.W., Platzer, W.J., 1999, Solar optical and infrared radiative properties of transparent polymer films. In: Proceedings of the 1999 ISES Solar World Congress, Jerusalem, Israel.

Wong, I.L., 2007. Optimum and Cost Effective Transparent Insulation Systems for Office Building Applications in Temperate and Tropical Climates, PhD thesis, University of Ulster, Northern Ireland.

Wong, I.L., Eames, P.C., Perera, R.S., 2007. A Review of Transparent Insulation Systems and the Evaluation of Payback Period for Building Applications. Solar Energy. 81(9), 1058-1071.